Excited State and Nonadiabatic Reaction Pathways Involving Single-Atom Impurities in Graphene

David Lingerfelt

7/28/2021

21st VISTA Seminar

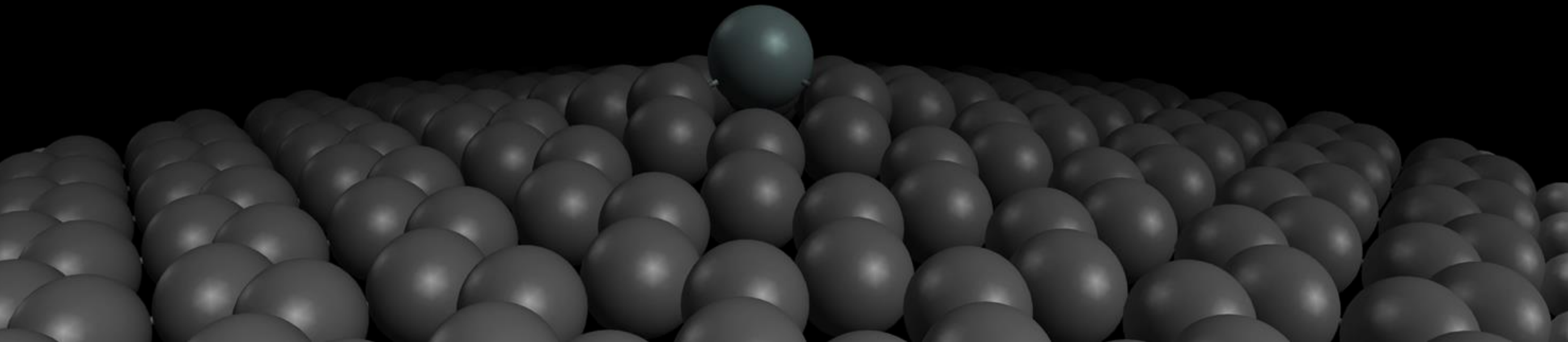

Acknowledgments

Prof. Tao Yu – UND
Dr. Anthony Yoshimura – LLNL
Dr. P. Ganesh - CNMS
Dr. Bobby Sumpter - CNMS
Dr. Jacek Jakowski - CSE

U.S. DEPARTMENT OF ENERGY | Office of Science

OAK RIDGE National Laboratory
CENTER FOR NANOPHASE MATERIALS SCIENCES

CADES

This work was performed at the Center for Nanophase Materials Sciences, a U.S. Department of Energy Office of Science User Facility.

Atomic Scale Manipulation with STEM

Aberration corrected optics allows focusing high energy (>>1keV) electron beams into sub-angstrom spot sizes.

Highly-localized response can induce chemical transformations on commensurate length scales.

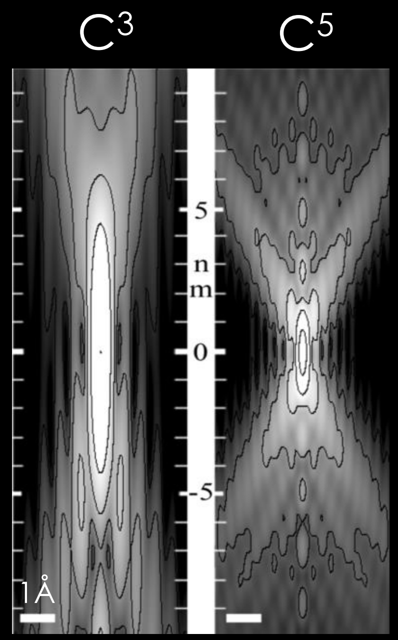

PNAS 2006, 103, 3044-3048

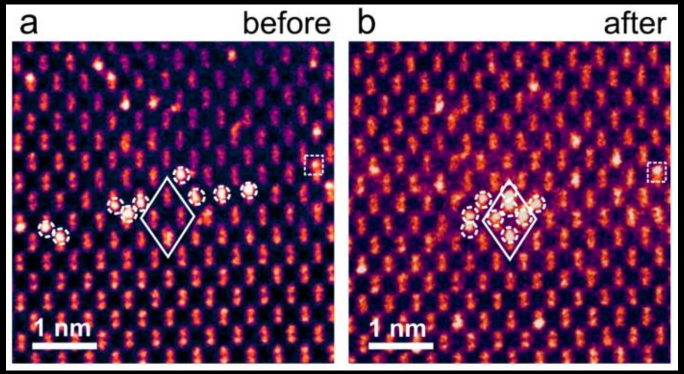

ACS Nano 2018, 12, 5873–5879

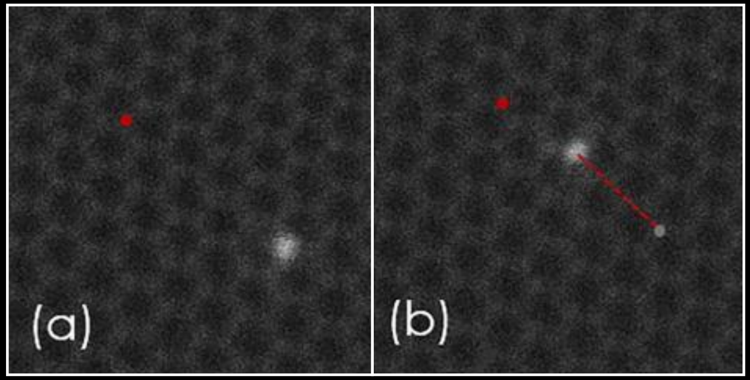

Appl. Phys. Lett. 2017, 111, 113104

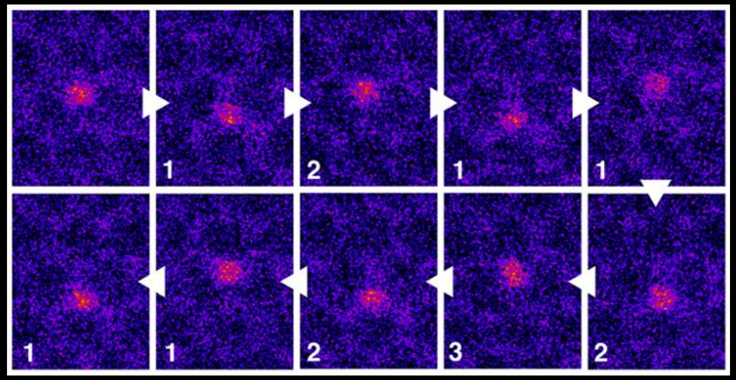

Nano Lett. 2018,18, 5319–5323

Structure of Si-C_3 defects in graphene

- Isovalent; belonging to period 3.
- Size mis-match leads to strain, alleviated by both in- and out-of-plane lattice distortion.
  - → pyramidalization about the Si atom
  - (Planar structure is a saddle point)

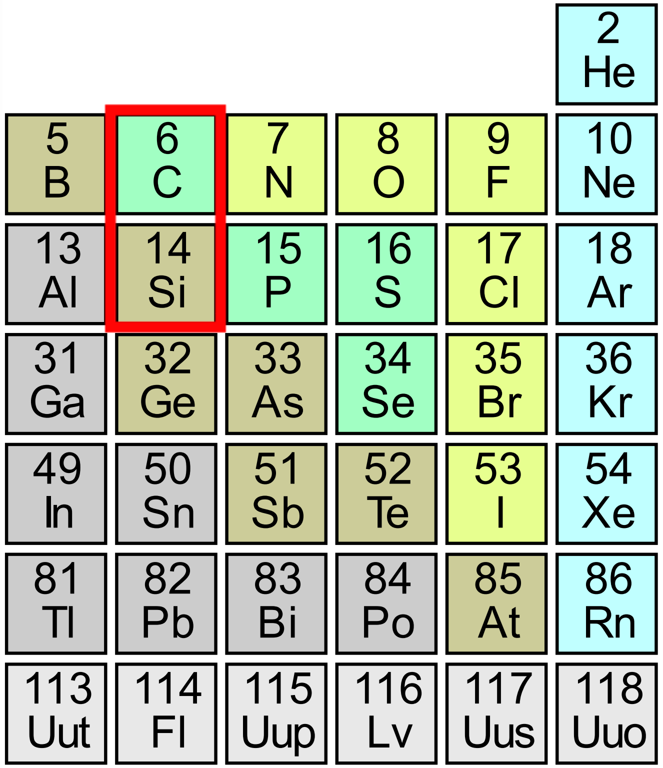

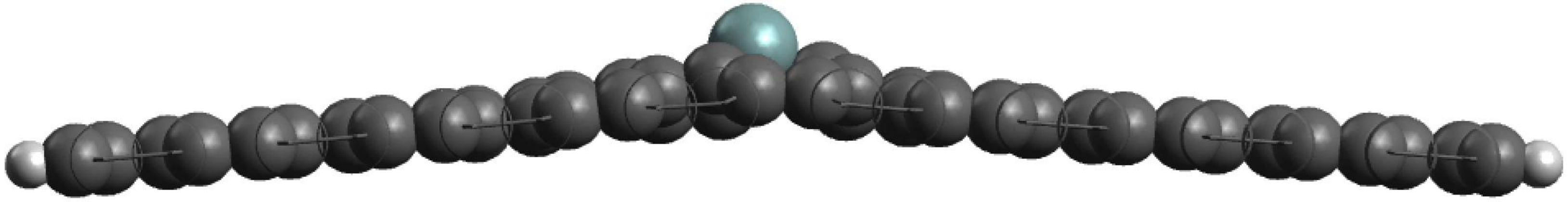

Strain and Pseudo Gauge Fields

Electromechanically deformed graphene "drumheads" show a pseudo-Landau level like progression in their STS→

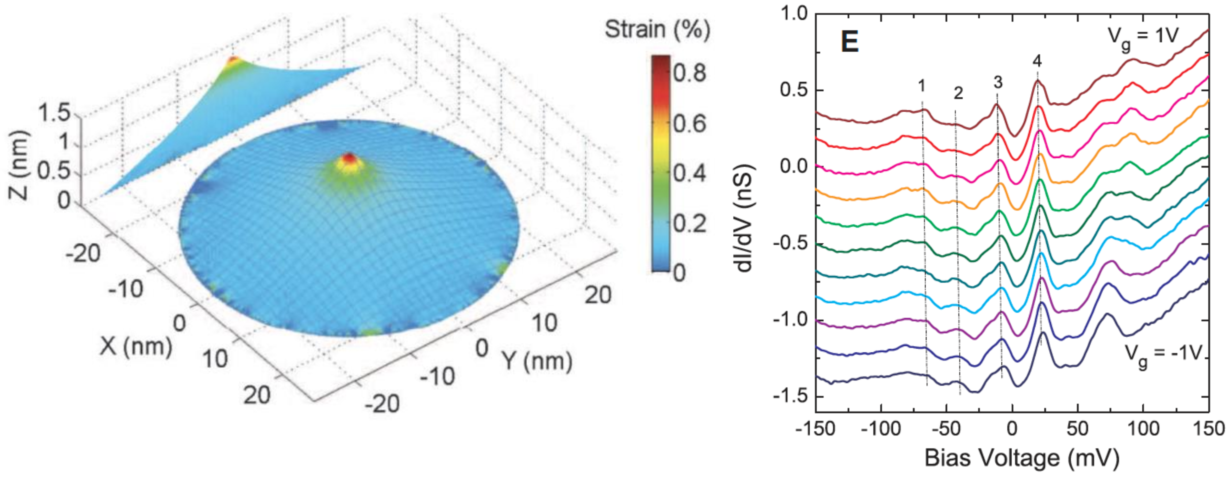

Science 2012, 336, 1557-1561.

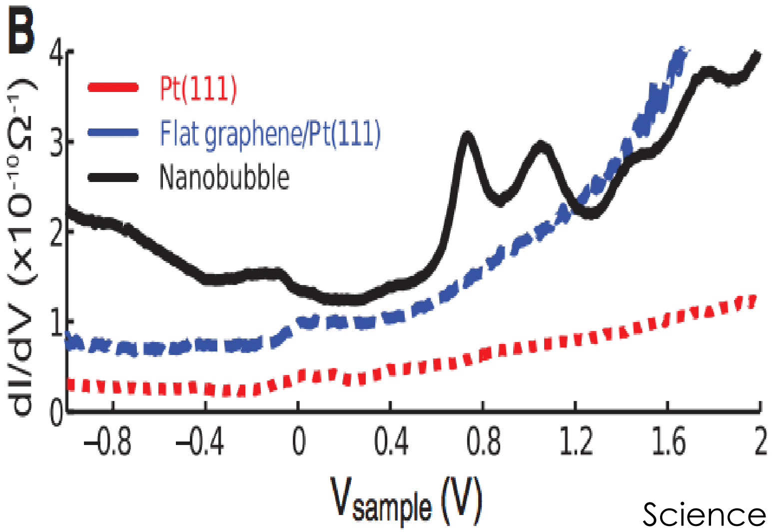

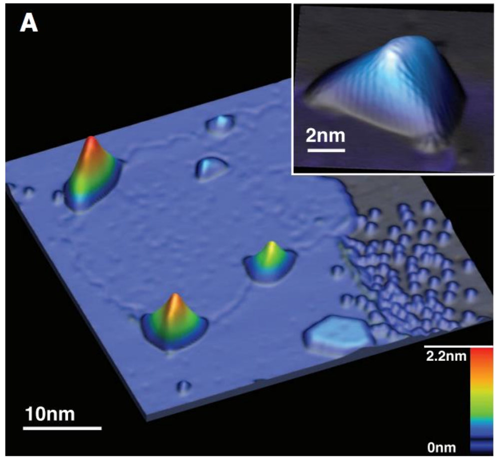

Science 2010, 329, 544-547.

← Similar story for CVD grown graphene nanobubbles on Pt

Si-C_3 diffusion in a graphene nanoflake

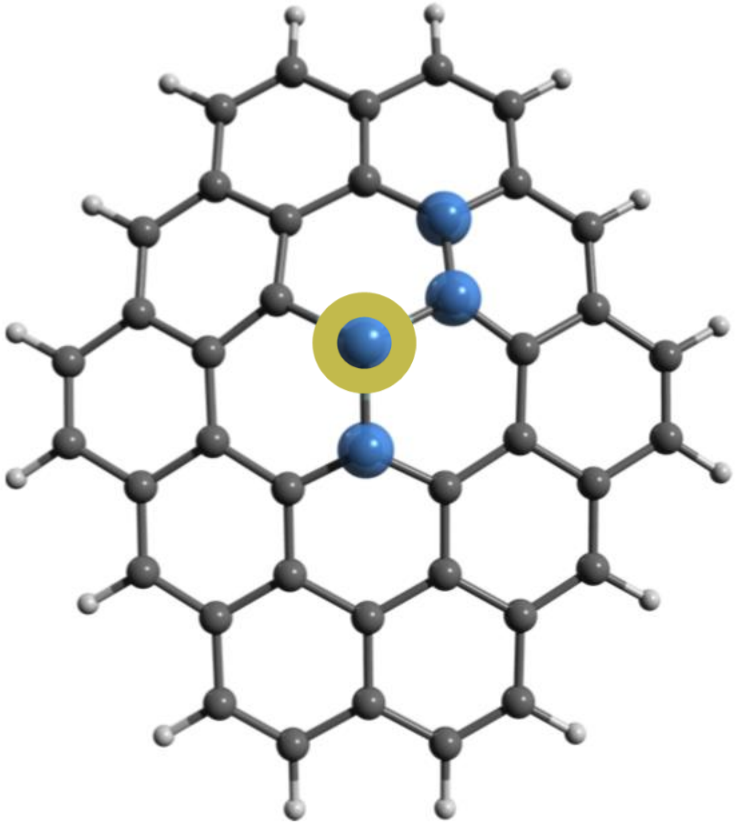

B3LYP/6-31g(d)

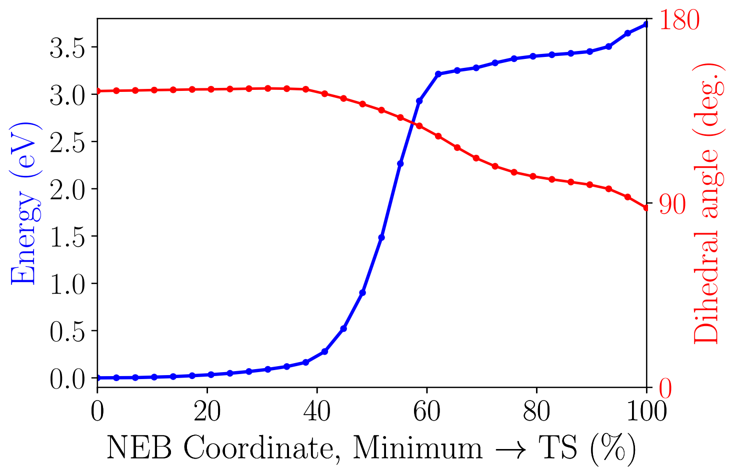

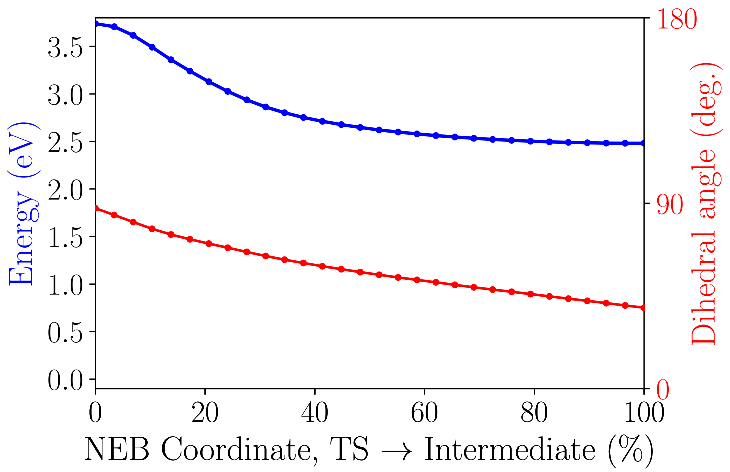

"Nonadiabatic Effects on Defect Diffusion in Silicon-Doped Nanographenes", D. B. Lingerfelt, T. Yu, A. Yoshimura, P. Ganesh, J. Jakowski, B.G. Sumpter. Nano Lett. 2021, 21, 236–242

Time-dependent density functional theory

(Linear Response)

$$\begin{bmatrix} \mathbf{A} & \mathbf{B} \\ \mathbf{B}^* & \mathbf{A}^* \end{bmatrix} \begin{bmatrix} \mathbf{X} \\ \mathbf{Y} \end{bmatrix} = \omega \begin{bmatrix} \mathbf{I} & \mathbf{0} \\ \mathbf{0} & -\mathbf{I} \end{bmatrix} \begin{bmatrix} \mathbf{X} \\ \mathbf{Y} \end{bmatrix}$$

$$A_{ia,jb} = \delta_{ij}\delta_{ab}(F_{aa} - F_{ii}) + (ia|jb) + (ia|f_{\text{xc}}|jb)$$

$$B_{ia,jb} = (ia|bj) + (ia|f_{\text{xc}}|bj)$$

$$\langle \Psi_0 | \hat{V}(\mathbf{r}_{\text{q}}) | \Psi_I \rangle = \sum_{ia} V_{ia}(\mathbf{r}_{\text{q}}) X_{ia}^I + V_{ai}(\mathbf{r}_{\text{q}}) Y_{ia}^I$$

$$\hat{V}(q, \mathbf{r}_{\text{q}}) = \frac{q}{|\hat{r} - \mathbf{r}_{\text{q}}|}$$

$$w_{0I}(\mathbf{r}_{\text{q}}) = 2\pi \left| \langle \Psi_0 | \hat{V}(\mathbf{r}_{\text{q}}) | \Psi_I \rangle \right|^2$$

("Real Time")

$$i \frac{\partial \mathbf{P}'(\mathbf{t})}{\partial t} = [\mathbf{F}'(t), \mathbf{P}'(t)]$$

$$\mathbf{P}'(t) = \mathbf{U}(t_0, t)\mathbf{P}'(t_0)\mathbf{U}^\dagger(t_0, t)$$

$$\mathbf{U}(t_0, t) = \mathcal{T} \exp\left(-i \int_{t_0}^{t} dt'\, \mathbf{F}(t')\right)$$

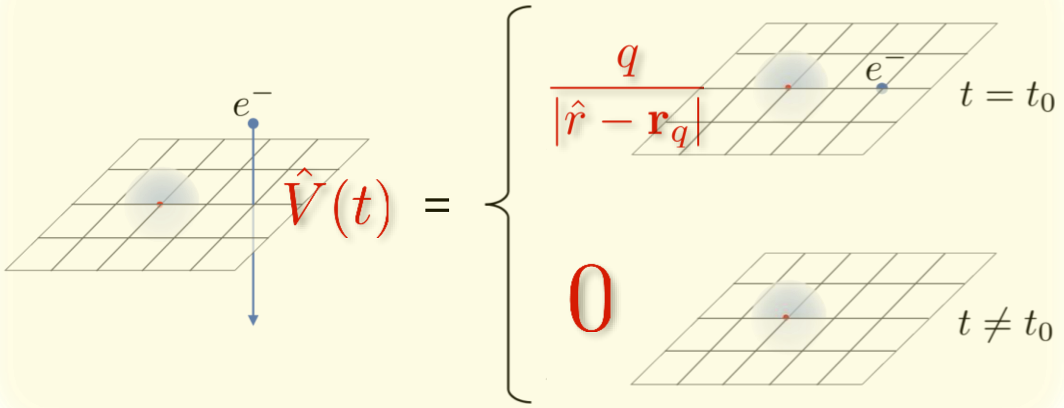

- Integrate EOM with 2nd order Magnus scheme (as implemented in NWChem)

Reaction profiles, nonadiabatic couplings, and $w_{0I}(\mathbf{r}_q)$

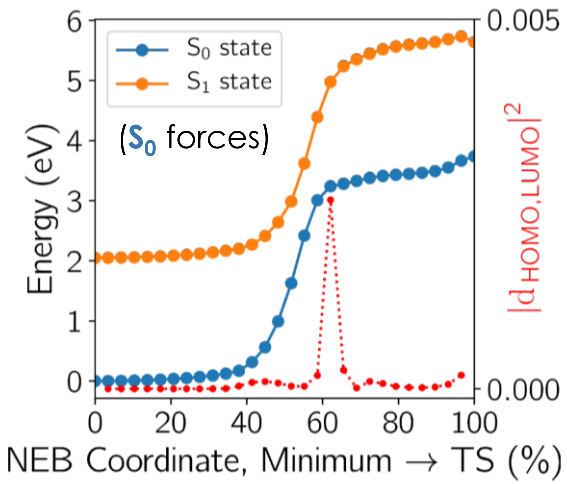

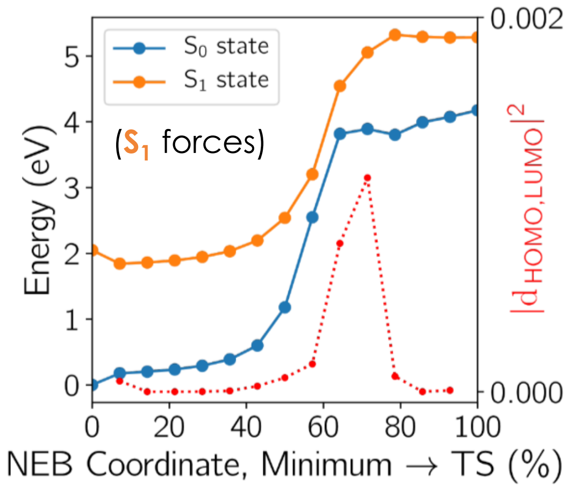

Minimum energy path

Direct Interchange, C_{2v} TS

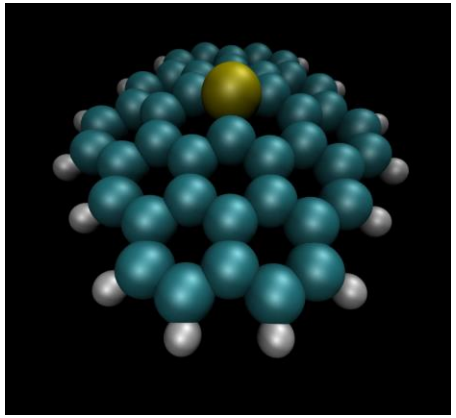

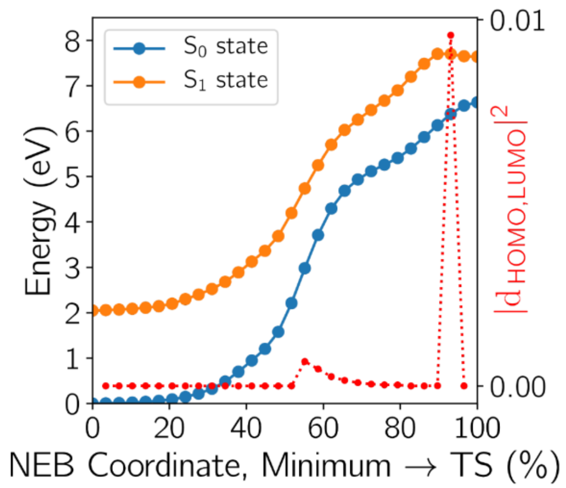

f_{01}= 0.1913

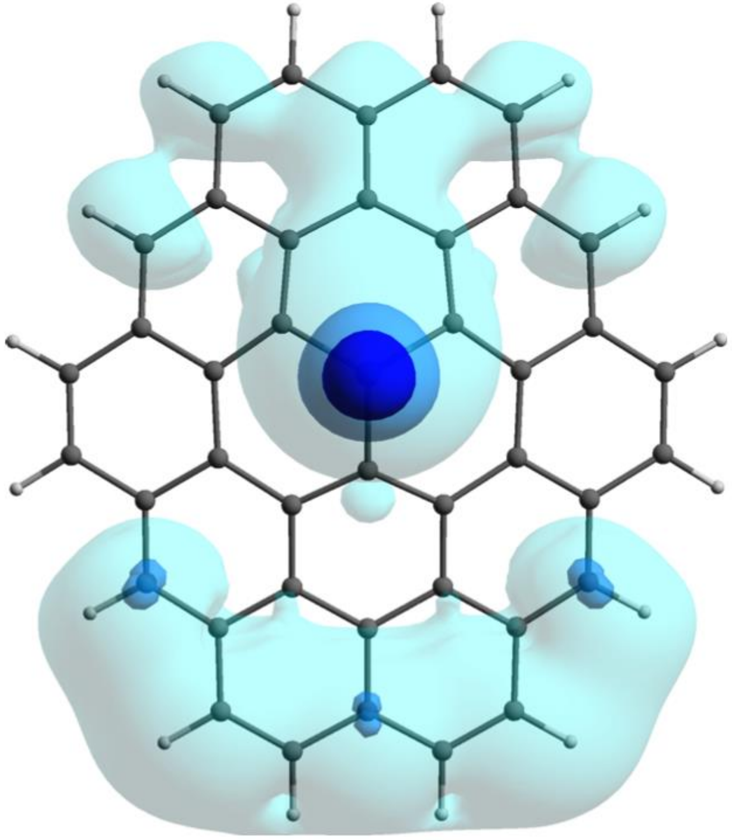

Excitation Rate
(isovalue= 0.001, 0.005, 0.01 AU^{-1})

Conclusions

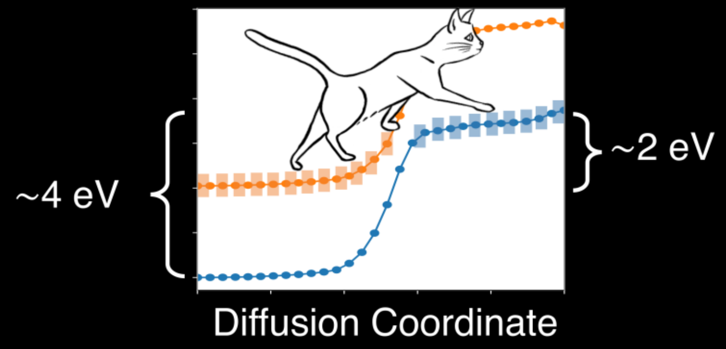

- $Si\text{-}C_3$ introduces defect-localized states that can be excited optically and through e-irradiation @ the defect site.
- Nonadiabatic coupling to lowest-lying defect-centered state can be strong along the diffusion coordinate.
- Nonadiabatic effects can send the effective diffusion barrier higher/lower depending on initial conditions.
- Disentangling the relative importance of these opposing effects will require coupled electronic and vibrational dynamics simulations.